Short pre-irradiation of TiO2 nanoparticles increases cytotoxicity on human lung coculture system

Ozge Kose, Maura Tomatis, Francesco Turci, Naila-Besma Belblidia, Jean-François Hochepied, Jérémie Pourchez, Valérie Forest

Short pre-irradiation of TiO_2 nanoparticles increases cytotoxicity on human lung coculture system

Ozge Kose[†], Maura Tomatis[‡], Francesco Turci[‡], Naila-Besma Belblidia[§,‖] Jean-François Hochepied[§,‖], Jérémie Pourchez[†], Valérie Forest[†*]

[†]Mines Saint-Etienne, Univ Lyon, Univ Jean Monnet, INSERM, U 1059 Sainbiose, Centre CIS, F-42023 Saint-Etienne, France

[‡]Dipartimento di Chimica and 'G. Scansetti' Interdepartmental Center for Studies on Asbestos and other Toxic Particulates, Università degli Studi di Torino, Torino, Italy

[§]Mines ParisTech, PSL Research University, MAT - Centre des matériaux, CNRS UMR 7633, BP 87 91003 Evry, France

[‖] ENSTA ParisTech UCP, Institut Polytechnique Paris, 828 bd des Maréchaux, 91762 Palaiseau cedex France

* **Corresponding author**: Valérie Forest:

Mines Saint-Etienne, 158 cours Fauriel, CS 62362, 42023 Saint-Etienne Cedex 2. FRANCE.

Email: vforest@emse.fr

Keywords

Titanium dioxide nanoparticles; UVA irradiation; cytotoxicity; pro-inflammatory response; reactive oxygen species; human lung coculture

Table of Content graphic

Abstract

Anatase titanium dioxide nanoparticles (TiO_2 NPs) are used in a large range of industrial applications mainly due to their photocatalytic properties. Before entering the lung, virtually all TiO_2 NPs are exposed to some UV light and lung toxicity of TiO_2 NPs might be influenced by photoexcitation that is known to alter TiO_2 surface properties. Although the TiO_2 NPs toxicity has been extensively investigated, limited data is available regarding the toxicity of TiO_2 NPs that have been pre-exposed to UV light, and their impact on humans remains unknown. In this study, five types of TiO_2 NPs with tailored physicochemical features were characterized and irradiated by UV for 30 min. Following irradiation, cytotoxicity, pro-inflammatory response, and oxidative stress on a human lung coculture system (A549 epithelial cells and macrophages differentiated from THP-1 cells) were assessed. The surface charge of all samples was less negative after UV irradiation of TiO_2 NPs and the average aggregate size was slightly increased. A higher cytotoxic effect was observed for pre-irradiated TiO_2 NPs compared to non-irradiated samples. Pre-irradiation of TiO_2 NPs had not a significant impact on the pro-inflammatory response and oxidative stress as shown by a similar production of IL-8, TNF-α and reactive oxygen species.

1. Introduction

Titanium dioxide nanoparticles (TiO_2 NPs), especially anatase form, are widely used in a large range of industrial applications in inks, plastic materials, ceramics, paper, foods, pharmaceutical and cosmetics due to their resistance to discoloration, high refractive index and photocatalytic activity. TiO_2 photocatalysis is a promising process and has attracted remarkable attention for the application of air and water purification [1–3].

Upon UV irradiation, photo-excited electrons migrate from TiO_2 bulk to surface, forming an electron/hole pair (e^-/h^+). In the presence of water and oxygen molecules, the electron/hole pair generates hydroxyl (OH•) or superoxide ($O_2•^-$) radicals which lead to the decomposition of a variety of organic and inorganic compounds [4,5]. This process may alter surface hydrophilicity and charge, may promote particle aggregation and enhance generation of reactive oxygen species (ROS) [6–8]. Some of these effects are transient (*e.g.*, ROS generation) and stop as soon as irradiation stops, whereas the changes in surface charge and particle aggregation persist over time [6] and may likely affect TiO_2 NPs' toxicity potential.

While some *in vitro* studies have shown that TiO_2 NPs reduce cell viability, increase ROS production and cytokine levels and cause genotoxicity even without light [9–11], several recent studies have shown that toxicity of TiO_2 is higher in the presence of UV light than in the dark [12–14]. Furthermore, several *in vivo* studies showed that TiO_2 NPs cause pulmonary inflammation, cell damage and oxidative DNA damage [15–17].

Sunlight reaching the Earth includes ca. 5% of UV radiation (315–400 nm, with a dose reaching the ground up to 0.1 W/cm^2) [18]. TiO_2 NPs in the environment are expected to be exposed to UV rays and possibly modified following photoexcitation. Due to the number of applications and the consequent environmental availability of TiO_2, inhalation of pre-irradiated TiO_2 NPs is likely the most common exposure route for humans. To the best of our knowledge, only one study [19] has been focused so far on the cellular effect induced by TiO_2 NPs preliminarily

exposed to UV light (pre-irradiated) for 24 hours and then incubated with cells in the dark. To assess whether short time of UV light exposure induces changes in the physicochemical properties and eventually affects TiO_2 NPs toxicity, we evaluated: (a) the changes of physicochemical properties caused by a short time UV irradiation on five samples differing in size, shape and surface charge, and (b) the toxicity in human lung coculture cells, before and after UV irradiation. To this purpose, we irradiated the samples for 30 min and we measured surface charge, aggregate size and the ability to generate free radicals in cell-free systems. Cytotoxicity, pro-inflammatory response (IL-8 and TNF-α release), and ROS generation were then evaluated on a coculture of human lung epithelial cells and macrophages differentiated from THP-1 monocytes.

2. Material and Methods

2.1 Synthesis and preparation of TiO_2 nanoparticle dispersion

In this study, we used four custom-made TiO_2 NPs with different and well-controlled properties and one commercially available P25 sample with a purity > 99.5% (Evonik P25 CAS: 1317-70-0, Sigma-Aldrich, Saint-Quentin-Fallavier, France). Evonik P25 TiO_2 was chosen for analysis as a reference particle due to its well-known photocatalytic activity [20] and it has been used in many tests as photocatalyst standard material by many studies [21,22].

Four TiO_2 NPs synthesis was performed using Chen *et al.* [23] method and they were named S1 to S4. Basically, titanium (IV) butoxide (CAS: 5593-70-4 reagent grade 97%, Sigma-Aldrich, Saint-Quentin-Fallavier, France) was mixed with triethanolamine (CAS: 102-71-6, analytical reagent 97%, VWR International, Fontenay-sous-Bois, France) in 1:2 molar ratio. The mixture was put in Teflon lined sealed and kept at a high temperature (150°C) for 24 h in autoclave. The pH of synthesis medium was adjusted by adding HCl or NH_4OH to tune particle size and morphology. Finally, the solutions were centrifuged three times and washed with deionized

water. The resulting products were dried in an oven at 40°C. Surface functionalization of S2 NPs was generated by aminopropyltriethoxysilane (APTES) using Zhao *et al.* [24] method and the functionalized nanoparticle labeled as S4. Their features are reported in Table 1. Stock suspensions of all NPs (1600 µg/mL) were prepared in deionized water (Milli-Q systems, Millipore) and sonicated with Branson Sonifier S-450 by cuphorn sonication in pulsed mode (2 s on/ 2 s off) for 10 min at 89 % amplitude. Before each experiment stock suspensions were sonicated for 15 min in a bath sonicator and vortexed vigorously diluted in culture medium, *i.e.* Dulbecco's Modified Eagle Medium (DMEM) containing 10% fetal bovine serum (FBS) to 15, 30, 60 and 120 µg/mL.

The amount of endotoxin present in the nanoparticle solutions was determined by the chromogenic method with a ToxinSensor Chromogenic Limulus Amebocyte Lysate (LAL) Endotoxin Assay kit (Genscript, Piscataway, Associates of Cape Cod Inc., Falmouth, MA, USA) according to the manufacturer's instructions. Endotoxin content was lower than the detection limit (0.001 endotoxin units per milliliter) in the nanoparticle samples. Therefore, samples did not show any endotoxin contamination.

2.2. Exposure to UV light

In the literature, studies using intensities of UVA light between 0.1 and 5 mW/cm^2 at a wavelength <380 nm reported that these conditions were sufficient to make TiO_2 NPs photoactive under realistic conditions [6,8,14,19,25]. In our study, the TiO_2 stock suspensions (1600 µg/mL in deionized water) were transferred into glass tubes and irradiated by UV light provided by a 100 W UV lamp (365 nm UV light, FV-97600-15 Cole-Parmer, Paris, France) for 30 minutes. The irradiation intensity was 1 mW/cm^2 as measured by a radiometer (Model PCE-UV34, PCE Instruments UK Ltd, Southampton, UK) simulating an indoor environment [26,27], and maximal irradiance of occupational exposure of UV [28]. The stock suspensions were diluted

in DMEM culture medium after the end of the UV irradiation of TiO_2 NPs and applied to the cells. The time from the end of the UV irradiation and the cell exposure was 15 min maximum.

2.3. Physicochemical characterization of TiO_2 nanoparticles

Size and shape were analyzed by transmission electron microscopy (TEM) using a FEI TECNAI 20FST operating at 200 kV and scanning electron microscopy (SEM) at 2-3 kV on a Zeiss Sigma 300 microscope using a secondary electron (SE) detector. Specific surface areas were measured by Brunauer, Emmett and Teller (BET) method (ASAP 2020 Volumetric Adsorption, Micrometrics, USA). Raman spectroscopy (Horiba Jobin–Yvon Xplora spectrometer) and X-ray powder diffraction (XRPD, Miniflex, Rigaku, Japan) techniques were used for the structural identification of the crystalline phases of NPs as reported in our previous study [29].

The spin trapping technique (5-5′- dimethyl-1-pirroline-N-oxide, DMPO, as trapping agent) associated to the electron spin resonance (ESR) spectroscopy (Miniscope 100 ESR spectrometer, Magnettech, Germany) was used to assess the radical formation from UV irradiated TiO_2 NPs in a cell free system. TiO_2 samples (120 µg/mL) were suspended in a buffered solution (potassium phosphate buffer 0.25 M, pH 7.4) containing 0.04 M DMPO or 0.04 M DMPO and 1 M sodium formate to detect hydroxyl and carboxyl radicals, respectively. ESR spectra were recorded on aliquot (50 µL) withdrawn after 30 min of UV irradiation and analyzed immediately. The instrument settings were as follows: microwave power 10 mW; modulation 1000 mG; scan range 120 G; center of field 3345 G. Blanks (negative controls) were performed with the same reaction mixtures without TiO_2. All experiments were repeated at least twice.

The hydrodynamic size and surface charge of pristine and irradiated TiO_2 NPs (120 µg/mL) in DI water and in DMEM were determined by using dynamic light scattering (DLS, Zetasizer

Nano ZS Malvern Instruments, Worcestershire, UK) and electrophoretic light scattering (ELS, Zetasizer Nano ZS Malvern Instruments, Worcestershire, UK).

2.4 *In vitro* toxicity study

2.4.1 Cell culture

The A549 human carcinoma epithelial cell line was supplied by the American Type Culture Collection (ATCC, CCL-185). A549 cells were grown in DMEM supplemented with 10% (v/v) FBS (S1810; Biowest, Nuaillé, France), 1% penicillin-streptomycin (VWR International, Fontenay-sous-Bois, France) and after reaching 80% confluency cells were trypsinized, washed with sterile phosphate-buffered saline (PBS) and centrifuged at 1500 g for 10 min and subcultured. The flasks were stored at 37°C in a humidified atmosphere with 5% CO_2.

The THP-1 human monocytic leukemia monocyte cell line (ATCC, TIB-202™) was a generous gift from Dr Ghislaine Lacroix from French National Institute for Industrial Environment and Risks (INERIS, France). THP-1 was cultured in Roswell Park Memorial Institute (RPMI) 1640 (Gibco, Life Technologies, Cergy-Pontoise, France) containing 10% FBS and 1% penicillin-streptomycin. THP-1 cells were counted with Trypan Blue regularly and subcultured usually twice a week. Subcultures were started with a cell concentration of 2 x 10^5 to 4 x 10^5 viable cells/mL and cells were maintained at a concentration between 10^5-10^6 cells/mL in suspension. THP-1 cells were maintained in a humidified atmosphere containing 5% CO_2 at 37°C. For the coculture, THP-1 cells were differentiated into mature macrophage-like cells in 96-well plate with 30 ng/mL of phorbol myristate acetate (PMA) (P1585, Sigma-Aldrich, Saint-Quentin-Fallavier, France) in RPMI for 24 h. After the incubation, cell surface was rinsed two times with DPBS. Then A549 cells were added on top of the differentiated THP-1 (at a ratio of one THP-1 to ten A549). These cocultured cells were

incubated in DMEM culture media at 37°C and 5% CO_2 for 24 h in a humidified incubator before the exposure to the pristine and 30 min irradiated TiO_2 samples.

2.4.2 Cell morphology

10^5 cells/well were seeded on 96 well plates. After 24 h exposure to the highest dose (120 µg/mL) of pristine and irradiated TiO_2 samples, the supernatant was discarded and cell surfaces were washed with PBS. After cells were observed using optical microscopy (Leica ICC50 HD, Leica Microsystems) at 40 x magnification and pictures were captured with the Moticam 1080 camera (Shimadzu, Japan).

2.4.3 Determination of cell viability

Cell viability was determined by Trypan blue exclusion assay since TiO_2 NPs have been reported to have interactions with MTT and XTT cytotoxicity assays [30]. 1.5 x 10^6 cells/well were plated onto 6-well microtiter plates in 1000 µL culture medium. Cells were exposed to 15, 30, 60 and 120 µg/mL of pristine and irradiated TiO_2 NPs. After incubation for 24 h at 37°C in a humidified incubator, the culture medium was removed, cells were washed with PBS and trypsinized. 20 µL cell suspensions were mixed with 80 µL Trypan blue dye to obtain 1:5 dilution and cells were counted under a microscope using Thoma cell counting chamber. Results are expressed as the mean ± standard error of the mean of three independent experiments and relative to control (unexposed) cells.

2.4.4 Pro-inflammatory response

10^5 cells/well were seeded on 96 well plates. Cells were exposed to 15, 30, 60 and 120 µg/mL of pristine and irradiated TiO_2 NPs. After 24 h exposure, the production of the pro-inflammatory markers tumor necrosis factor alpha (TNF-α), and interleukin 8 (IL-8) were determined by

sandwich enzyme-linked immunosorbent assay (Quantikine Human TNF-α, and Quantikine Human IL-8 Immunoassay; R&D Systems, Lille, France) according to the manufacturer's instructions. The optical density of each sample was determined using a microplate reader (Multiskan RC; Thermo Labsystems, Helsinki, Finland) set to 450 nm. Three independent experiments were performed, and the production of TNF-α and IL-8 was reported to that of control (unexposed) cells.

2.4.5 Determination of Reactive Oxygen Species (ROS) production

Coculture cells were seeded in 96 well black polystyrene microplates (10^5 cells/well) and were exposed to 15, 30, 60 and 120 μg/mL pristine and irradiated TiO_2 NPs. After 90 min and 24 h exposure, the level of ROS was determined using the OxiSelect kit from Cell Bio Labs (San Diego, CA) according to the manufacturer's instructions. The assay employs the cell-permeable fluorogenic probe 2', 7'-Dichlorodihydrofluorescin diacetate (DCFH-DA). Fluorescence was detected using a Fluoroskan Ascent fluorometer (excitation: 480 nm, emission: 530 nm, Thermo Labsystems), and the generation of ROS was reported to that control (unexposed) cells.

2.5 Statistical analyses

Statistical analyses were performed using GraphPad Prism® (version 8.0, GraphPad Software, San Diego, CA, USA). All data were presented as the mean ± the standard error of the mean (SEM). Differences were considered to be statistically significant when P value was < 0.05. One-way Anova Tukey test analysis was performed for comparison between control and experimental groups and between pristine and irradiated groups.

3. Results

3.1 Physicochemical features

The toxicity-relevant physicochemical features of the TiO_2 NPs used in this study are reported in Tables 1, 2 and Figure 1.

Table 1. Particle primary size (TEM), specific surface area (SSA, BET), particle shape (TEM, SEM), and crystal structure (XRPD) of the TiO_2 NPs. [a] minimum and maximum Feret diameters; [b] APTES coating was carried out on S2-type NPs to obtain S4 NPs.

	S1	S2	S3	S4	P25
Primary size (nm)	15	30	20 – 250[a]	30	21
SSA (m^2/g)	146	61	41	61	55
Particle Shape	Spherical	Spherical	Rod	Spherical	Spherical
Crystal structure	Anatase	Anatase	Anatase	Anatase	Anatase: Rutile (90:10)
Surface coating	No	No	No	APTES[b]	No

The radical generation through UV irradiation of different types of TiO_2 in buffer solution was explored. UV irradiation of suspension of TiO_2 in the presence of DMPO produced the DMPO-HO• and DMPO-CO_2•$^-$ adducts as shown in Figure 1 a and 1 b, respectively.

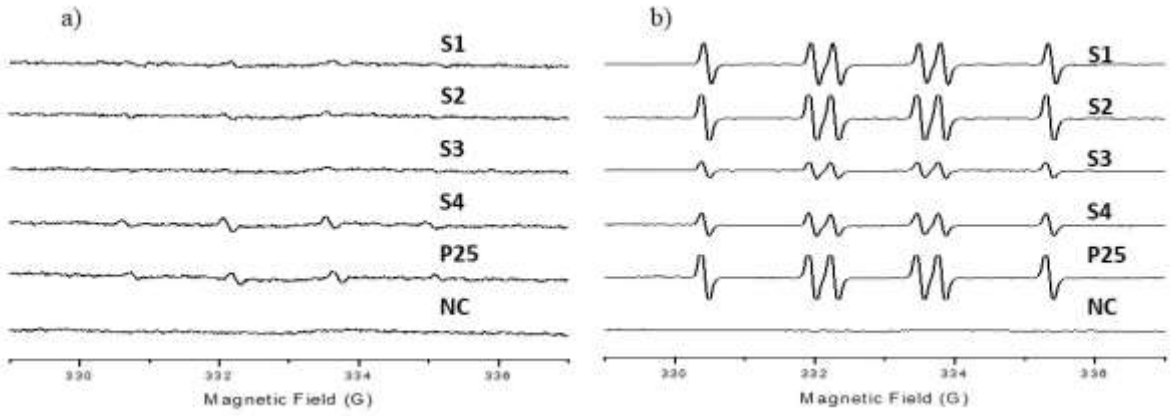

Figure 1. Generation of HO• and $CO_2^{\bullet-}$ radicals from suspensions of TiO_2 NPs (120 µg/mL) under irradiation with UV light. EPR spectra of (a) DMPO-HO• and (b) DMPO-$CO_2^{\bullet-}$ adducts. Negative Control (NC) corresponds to buffer solution without particles. The number of radicals produced is proportional to the intensity of the ESR signal.

Regarding hydroxyl radical formation, negligible traces of HO• radicals were observed at 30 min UV irradiation for S1, S2 and S3, whereas weak signals of the DMPO-HO• adduct were detected for S4 and P25. Although HO• is frequently assigned to the major reactant responsible for the photo-oxidative activity of TiO_2, the observed weak HO• signal might be due to the low concentration of the particle suspensions. However, as illustrated in Figure 1b characteristic peaks of DMPO-$CO_2^{\bullet-}$ were observed in all the irradiated suspensions of TiO_2 and the intensity was higher for S1, S2, and P25 than S3 and S4. As shown in our previous study [29], no DMPO-HO• and DMPO-$CO_2^{\bullet-}$ signals were observed for the pristine TiO_2 samples.

To verify whether short-time UV-irradiation modifies toxicologically-relevant properties of TiO_2, we compared the size of particle aggregates and the surface charge of pristine and irradiated TiO_2 NPs in deionized water and in 10% FBS supplemented DMEM (Table 2).

Table 2. Average hydroynamic size[a], polydispersity index (PDI)[b] and Zeta potential of pristine and UV irradiated TiO_2 NPs (120 µg/mL) in deionized water (DI H_2O) and in DMEM (10% FBS). All data are presented as mean of three independent characterizations ± SD. [a] Dynamic light scattering (DLS) measurements are the mean of at least 3 runs each containing 20 sub-measurements.

Pristine TiO_2 (in DI H_2O)		UV irradiated TiO_2 (in DI H_2O)		Pristine TiO_2 (in DMEM)		UV Irradiated TiO_2 (in DMEM)	
Average hydroynamic	**Zeta Potential**	**Average hydroynamic**	**Zeta Potential**	**Average hydroynamic**	**Zeta Potential**	**Average hydroynamic**	**Zeta Potential**

	size[a] (PDI,nm)	(mV) @pH 7.5	size[a] (PDI,nm)	(mV) @pH 7.5	size[a] (PDI,nm)	(mV) @pH 7.5	size[a] (PDI,nm)	(mV) @pH 7.5
S1	211.4 ± 2.3 (0.145)	-13.2 ±4.2	321 ± 28.3 (0.415)	-9.01 ± 0.7	226 ± 9.1 (0.282)	-33.8 ± 1.8	292.1 ± 3.5 (0.234)	-8.0 ± 0.7
S2	969.3 ± 39.5 (0.266)	-13.8 ±4.4	1531 ± 406 (0.136)	-8.36 ±0.4	1094 ± 46.4 (0.364)	-32.6 ± 1.7	1149 ± 38.6 (0.475)	-5.3 ± 1.2
S3	1409 ± 89.6 (0.114)	-15.8 ±4.0	1795 ± 346.4 (0.545)	-7.04 ±0.8	1275 ± 66.6 (0.179)	-33.7 ± 3.5	1299 ± 112.1 (0.714)	-7.5 ± 0.6
S4	1204 ± 59.9 (0.160)	+12.3 ±0.5	1231 ± 143.8 (0.504)	-8.4 ±0.2	1398 ± 54.9 (0.475)	-36.4 ± 3.5	1433 ± 133.1 (0.308)	-9.9 ± 0.2
P25	256.4 ± 136.6 (0.272)	-15.2 ±5.3	410 ± 5.1 (0.383)	-9.95 ±1.6	325 ± 4.1 (0.260)	-33.1 ± 1.7	353.6 ± 3.45 (0.256)	-7.7 ± 0.7

In DI water, all samples but S4 were negatively charged. The positive surface charge of S4 is due to the presence of amine groups (-NH_2) of APTES functionalization. UV irradiation induced the TiO_2 NP surface to be less negative and the average hydrodynamic size of particles was increased indicating some further particle aggregation.

In DMEM (10% FBS), also APTES-functionalized S4 NPs acquired a negative charge at pH 7.5, likely due to adsorption of media components, as previously observed for TiO_2 NPs [31]. UV irradiation caused a marked decrease of the negative zeta potential towards less negative values also in DMEM. Specifically, the zeta potential of pristine NPs ranged between -31 mV and -36.6 mV and decreased to -9.9 mV to -5.3 mV after irradiation.

3.5. Cell morphology

The morphology of coculture cells after 24 h exposure to the highest dose (120 µg/mL) of pristine and irradiated TiO_2 NPs were illustrated in Figure 2.

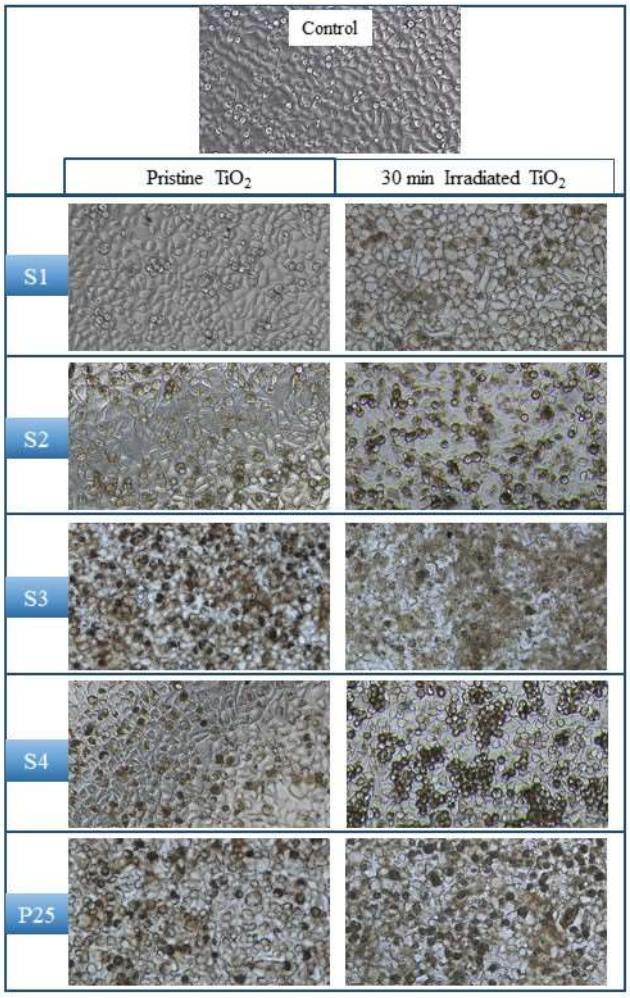

Figure 2. Microscopic images of coculture cells (A549 + macrophages differentiated from THP-1 cells) exposed to 120 µg/mL pristine and 30 min irradiated TiO_2 NPs for 24 h (40 x magnification). Control cells (unexposed to NPs).

The control (untreated) cells show the original morphology of epithelial A549 and macrophages differentiated from THP-1 cells. Most of the control cells were adherent to the culture flask. However after exposure to pristine and irradiated TiO_2 NPs, the cell morphology was considerably changed compared to control cells. Cell shrinkage, and loss of contact with adjacent cells were observed. Also, loss of cellular adhesion to the substrate was observed and most of the cells detached from the surface of the culture flask and appeared floating in the

culture medium. The cell morphological changes induced by irradiated NPs were more pronounced than those induced by pristine NPs.

3.2. Cytotoxicity

Cytotoxicity induced by pristine and irradiated TiO_2 NPs on coculture cells (A549 + macrophages differentiated from THP-1 cells) are presented in Figure 3.

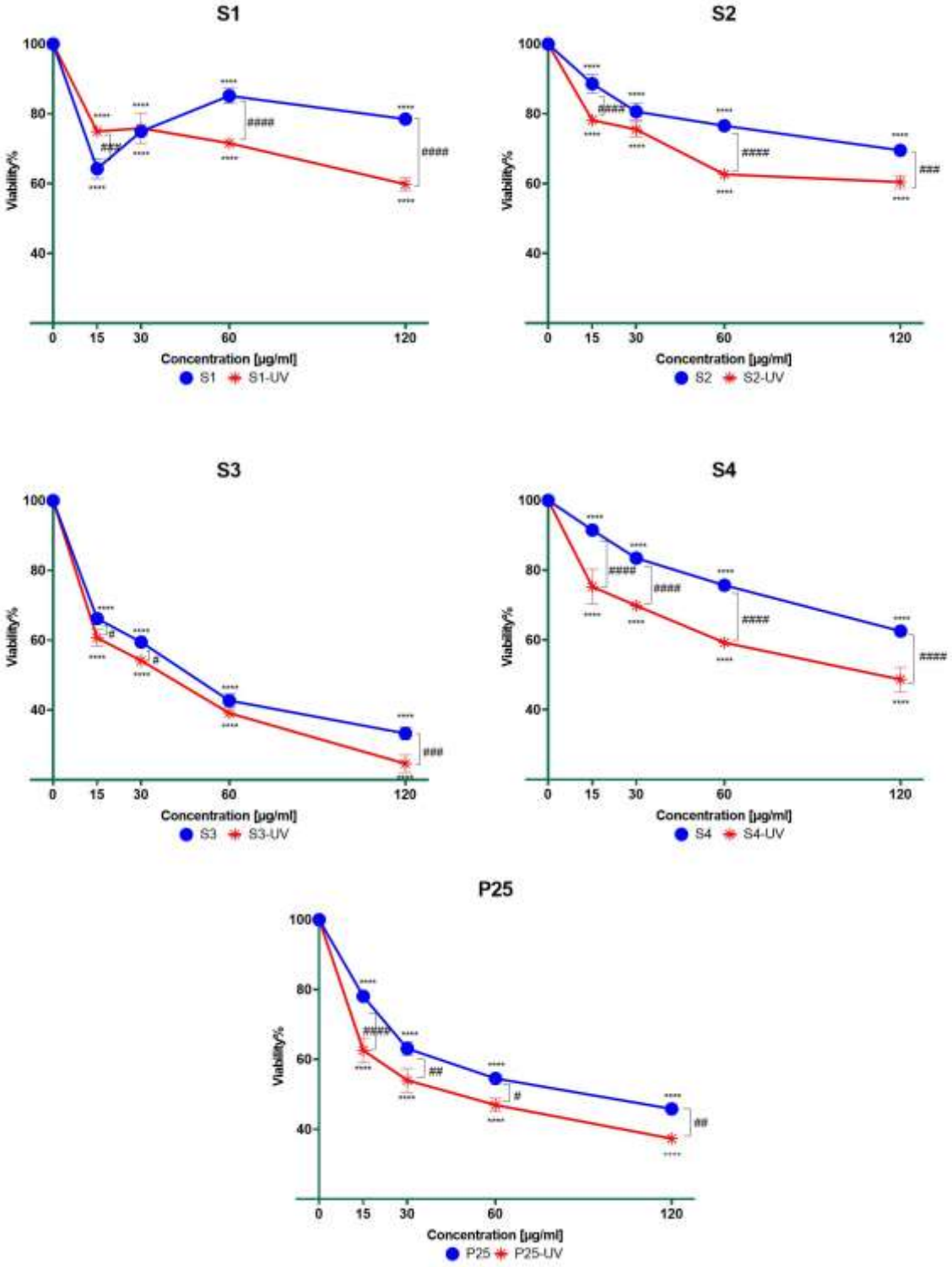

Figure 3. Cell viability assessed by Trypan blue assay 24 h after coculture cells (A549 + macrophages differentiated from THP-1 cells) were exposed to pristine and irradiated TiO_2 NPs at the indicated concentrations. Values are the mean ± SEM of three independent experiments. Statistically different from control (****) P<0.0001. Statistical difference between pristine and

irradiated samples ($^{\#}$) $P < 0.5$ ($^{\#\#}$) $P < 0.01$, ($^{\#\#\#}$) $P < 0.001$, (####) $P < 0.0001$. Statistical analyses were conducted using one-way Anova analyses and Tukey's multiple comparison test.

Considering the exposure to pristine TiO_2 NPs, the cell viability decreased in a dose-dependent manner in all samples except S1 compared to control. The maximal cell loss was observed for rod shaped S3 treated cells starting from the lowest doses (15 μg/mL). At the highest concentration (120 μg/mL), cell viability was found to be 33.3 % for S3. P25, on the other hand, caused 45.8% cell viability at the highest concentrations, while cell viability was found to be 78.5%, 69.5% and 62.5%, for S1, S2 and S4, respectively.

Exposure to irradiated samples caused a dose-dependent decrease in cell viability compared to the control group and showed a statistically significant difference at all the tested concentrations ($P < 0.0001$, all). Irradiated rod shaped S3 and P25 caused the highest cytotoxic effects and this effect was more pronounced at the highest doses (24.6% and 37% at 120 μg/mL, respectively). The comparison of toxicities induced by pristine and irradiated TiO_2 NPs highlighted a significant increase of cytotoxicity when all particles at all tested concentrations were pre-exposed to UV light, and few negligible exceptions to this trend were observed. The only relevant exception is caused by pristine S1, likely due to the agglomeration of the smallest NP investigated in this work used at the highest doses.

3.3. Pro-inflammatory response

Since IL-8 and TNF-α are major pro-inflammatory mediators in lung epithelial cells and macrophages respectively [32] we examined whether TiO_2 samples induced IL-8 and TNF-α production in coculture (A549 + macrophages differentiated from THP-1 cells). Results are reported in Figure 4.

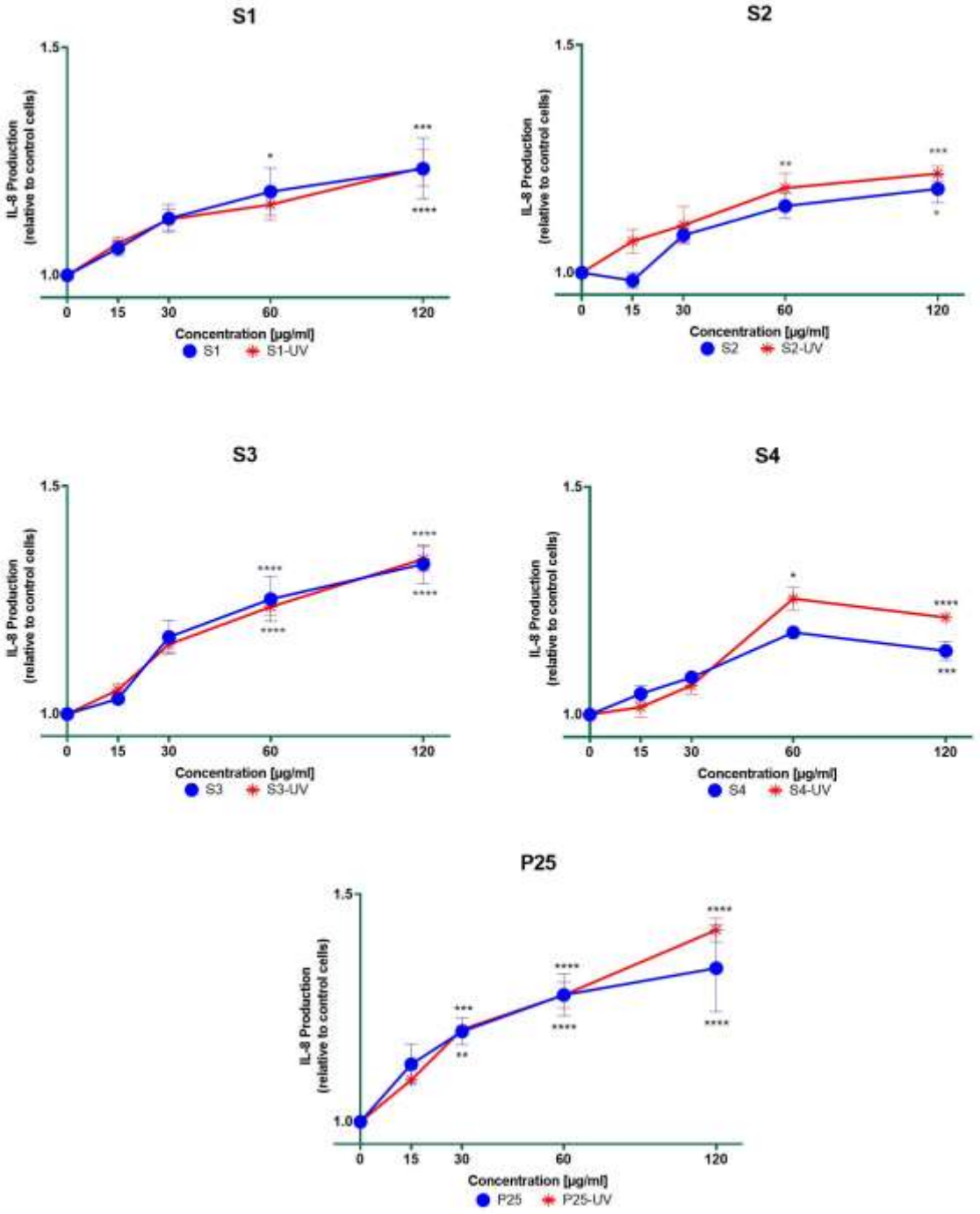

Figure 4. IL-8 production after 24 h exposure to the indicated concentrations of pristine and irradiated TiO_2 NPs in coculture cells (A549 + macrophages differentiated from THP-1 cells). Values are the mean ± SEM of three independent experiments. Statistically different from control (*) $P < 0.5$, (**) $P < 0.01$, (***) $P < 0.001$, (****) $P < 0.0001$. Statistical analyses were conducted using one-way Anova analyses and Tukey's multiple comparison test.

Regarding IL-8 production, all pristine TiO_2 samples caused a dose-dependent increase compared to the control group. A higher production was observed significantly for S3 and P25 at 60 μg/mL ($P < 0.0001$) and at the highest dose (120 μg/mL, $P < 0.0001$). Similarly, IL-8 release from coculture was enhanced after exposure to irradiated samples whereas this increased production was almost the same as that observed for the pristine samples (no statistically significant difference). Similarly, UV irradiated or pristine TiO_2 NPs did not cause significant TNF-α production compared to the control group and there were no significant differences between pristine and irradiated samples (data not shown).

3.4. Determination of reactive oxygen species (ROS) production

Pristine and irradiated TiO_2 NPs did not induce significant ROS production in coculture compared to the control group (unexposed to TiO_2 NPs) whatever the time of analysis (90 min or 24 h). No statistically significant difference was observed between pristine and irradiated TiO_2 NPs (data not shown).

4. Discussion

There is great interest in applying semiconductor materials in a variety of applications, especially TiO_2 has attracted attention in water treatment, air purification, self-cleaning surfaces due to its photocatalytic activity [5]. Considering the transititon of TiO_2 into a photoactive state under sunlight, toxicity caused by inhalation of photoactivated TiO_2 NPs should be taken into consideration.

Changes in the chemical or physical structure of TiO_2 due to the UV irradiation are important to consider with respect to their environmental fate and toxicity in humans. After irradiation the

markedly negative surface charge of all TiO_2 NPs was less negative and shifted towards zeta potential values ranging from -33 to -7.5 mV.

Long (50 h) UV irradiation of TiO_2 NPs is known to induce the generation of a large number of bridging hydroxyl species that are characterized by a strong acidic character (pK_a 2.9). On the contrary, terminal hydroxyl species (≡Ti – OH) are rather alcaline (pK_a = 12.7) and their presence favours a more neutral surface charge in physiological media. We might speculate that the short irradiation time used in this and other works [6] may favour these latter species, as the former ones, more thermodynamically stable, require that water molecules replace oxygens that are ejected during the h^+-driven oxidation of O_2^- anions. An excess of terminal hydroxyl species upon short time irradiation could be at the basis of the less negative surface charge observed for all the irradiated TiO_2 NPs.

These results are in good agreement with a number of other studies showing the physicochemical properties of TiO_2 have changed with UV irradiation [6,7,19,33]. The extent to which these changes induces differences in their *in vitro* toxicity is shown in the present study. *In vitro* cytotoxicity assay revealed that pristine TiO_2 NPs caused a significant reduction in cell viability compared to the control group (Figure 3). The cytotoxic potential of TiO_2 NPs after UV irradiation was increased compared to pristine NPs and this is consistent with observations of cell morphology (Figure 2). This latter only allowed us to observe cell shrinkage, cell detachment which are signs that cells are dying, however, to really appreciate the nature of cell death (apoptosis, necrosis) further experiments must be carried out. Similarly, to better understand why pre-irradiated nanoparticles induced more morphological changes than pristine nanoparticles, further studies should be conducted to better characterize the underlying mechanisms. In some studies, it has been shown that UV irradiated TiO_2 NPs reduce cell viability more than non-irradiated TiO_2 NPs [12,14,34] , but only one study focused on the effect of TiO_2 pre-irradiation on cell viability[19]. In this study [19], the effect of 24 h UV pre-irradiated 18

nm and 105 nm anatase TiO_2 NPs on the cell viability of human liver cancer cell line (Hep G2) was investigated. Our results share a number of similarities with Petkovic *et al.*[19] findings that UV pre-irradiation caused more cell viability reduction than pristine TiO_2 NPs and 24 h pre-irradiation caused changes on particle surface charge. Remarkably, our data indicate that even a 30 min short term UV irradiation is able to alter TiO_2 toxicologically relevant features, such as surface charge and aggregate size, and thus modulate its cytotoxicity.

Also, it has been shown in RAW 267.4 cells that near-visible light activation of TiO_2 NPs induced cytotoxicity [35,36]. It was suggested that, the hydroxyl radicals generated upon photo-activation and the ROS-mediated damages to the surface-adsorbed biomolecules could be responsible for the cytotoxicity of photo-activated TiO_2 NPs [35]. Using Fe-doped TiO_2 NPs George *et al.* [36] showed that the band gap energy decreased with increasing levels of Fe loading, this reduction was associated to an enhanced oxidant injury and cell death. These results illustrate the importance of band gap energy in the cell response to phototoxic TiO_2 NPs and call for caution about the adverse effects these NPs may generate in humans and the environment during high-intensity light exposure. On the other hand Xiong *et al.* [35] further investigated the influence of the generation of hydroxyl radicals on poly(ethylene-alt-maleic anhydride) (PEMA) and chitosan-coated TiO_2 NPs. The results indicated a reduced cell toxicity triggered by coated TiO_2 NPs after photo-activation, by hindering adsorption of biomolecules and generation of hydroxyl radical during photo-activation. With this understanding, we can find ways to modify the photo-toxicity of TiO_2 NPs and design safer nanomaterials.

Regarding pro-inflammatory responses, in our study both pristine and irradiated TiO_2 NPs caused significantly IL-8 production only at the high doses (60, 120 µg/mL) compared to control group whereas there were no significant differences between pristine and irradiated samples (less negative surface charge) showing that UV pre-irradiation had no effect on the pro-inflammatory responses. The results of pristine TiO_2 NPs IL-8 production were consistent

with Dekali *et al.*'s findings [37]. In this study, the inflammatory effect of the anatase TiO_2 NPs ($\leq$ 25 nm, 200-220 m^2/g) was tested on the coculture (A549+THP-1) model. An increased IL-8 production was detected although no significant changes were observed in the production of TNF-α after TiO_2 NPs exposure. In the literature, the studies examining the pro-inflammatory responses of TiO_2 and photo-active TiO_2 NPs on the coculture system are limited. This makes it difficult to compare studies and draw conclusions.

Inflammation and oxidative stress are closely related processes that work interdependently [38]. Oxidative stress triggers inflammation, or if inflammation occurs first, oxidative stress develops, which further exacerbates inflammation [39]. In this study, TiO_2 NPs had an impact on the pro-inflammatory responses but surprisingly pristine or irradiated TiO_2 NPs did not trigger significant ROS production in coculture compared to the control group (unexposed to TiO_2 NPs). Especially considering the P25 used as a reference substance in this study, the effects of P25 on oxidative stress are contradictory in the studies[40,41] as assessed by the DCFH-DA assay. The reason for the absence of oxidative stress upon treatment with pristine or irradiated TiO_2 NPs might be the possible interference by the NPs with the DCF in DCFH-DA ROS assay which could hinder the traceability chain by quenching the fluorescent signal. An unintended bias should be taken into consideration. Besides, considering the cell lines used in this study, alveolar macrophages are also equipped with a well-advanced defence system of enzymatic and non-enzymatic antioxidants, which are known scavengers of ROS [42,43]. Thus, radical scavengers present in the cells may significantly protect them from UV irradiated or pristine TiO_2 induced ROS production. This must be confirmed by a comprehensive study of oxidative stress also including the assessment of anti-oxidant system induction.

Regarding photoactivity, our ESR results showed that UV irradiation of TiO_2 NPs resulted in acellular production of $CO_2^{\bullet -}$ and much less HO• production without significant change in oxidative stress, although many studies showed that the free radical generation triggered

cellular oxidative stress [12,44,45]. This may not be assumed in our study because after the particles were exposed to UV irradiation, they were incubated with the cells in a dark environment (*i.e.* incubator), where there was no UV light. When UV light irradiation is ceased, the rapid recombination between electron–hole pairs stops the photocatalytic activity of TiO_2 [46], however, the free radicals generated, to stabilize their unpaired electrons, could attack nucleic acids, proteins, lipids, *etc.* potentially altering the functions of these biomolecules, leading to biological outcomes.

In line with the investigation of potential links between cytotoxic effects of irradiated TiO_2 NPs and changes of physicochemical properties, we showed that the irradiated NPs have less negative surface charge compared to the pristine particles, creating more cytotoxicity. The magnitude of the negative zeta potential decreased by UV irradiation, the reducing electrostatic barrier could increase the chances of cell-particle interactions and result in higher toxicity. As reported by Jeon *et al.* [47], less negatively charged NPs are more efficiently taken up by THP-1 macrophages.

Besides, the surface charge is a parameter involved in the formation of the protein corona. For example, one study [48] showed that total serum protein, BSA and apolipoprotein 1 amounts adsorbed to silica NPs decreased with an increase in negative charge density. Consequently, proteins contained in the cell culture medium can adsorb differently at the altered NP surface (*i.e.* there is a different corona) [49]. It is known that the protein corona has an impact on the internalization of NPs by cells and thus potentially on the cytotoxicity induced [50–52]. This assumption is supported by a slight change in the average aggregate size of the particles before and after irradiation and an altered surface charge. Further study is necessary to better understand if the protein corona may play a role and it is the topic of our current research.

Besides the comparison of the pristine and pre-irradiated nanoparticle toxicity, it is worth noting that since five nanoparticle types differing in their physicochemical properties were used in this

study, we were able to conclude on the influence of these features on the biological response. As reported in our previous study, the toxicity induced by pristine nanoparticles was higher with bigger primary sized, less agglomerated, rod-shaped and positively charged nanoparticles. After 30 min of UV irradiation, no change was observed on the toxicity ranking of the influence of these physicochemical properties. These findings may be useful for the safer-by-design development of TiO_2 NPs.

Conclusion

In conclusion, the results of this study showed that irradiated TiO_2 NPs induced a higher cytotoxic effect than the pristine TiO_2 NPs on human lung cells in relation to an altered surface charge. Irradiated TiO_2 NPs caused a pro-inflammatory response in the same incidence as pristine NPs therefore it cannot be claimed that UV irradiation has an effect on the pro-inflammatory response. No impact was observed on ROS production neither in pristine nor in irradiated TiO_2 NPs treated cells. However further investigations are needed. Since it is possible for the TiO_2 in the environment to be photoactivated by sunlight, the risk assessment of photoactive TiO_2 NPs should be taken into account. In this sense, the results of this study contribute to the toxicological evaluation of TiO_2 NPs and photoactive TiO_2 NPs in human lung cells.

Funding

This research did not receive any specific grant from funding agencies in the public, commercial, or not-for-profit sectors.

Acknowledgments

We would like to thank Dr. Ingrid Corazzari for the kind support in physicochemical characterization of the TiO_2 NPs. Ozge Kose acknowledges the support of the "G. Scansetti" Center of the University of Torino for partially funding her international secondment.

References

(1) Ziental, D.; Czarczynska-Goslinska, B.; Mlynarczyk, D. T.; Glowacka-Sobotta, A.; Stanisz, B.; Goslinski, T.; Sobotta, L. Titanium Dioxide Nanoparticles: Prospects and Applications in Medicine. *Nanomaterials* **2020**, *10* (2), 387. https://doi.org/10.3390/nano10020387.

(2) Chen, X.; Selloni, A. Introduction: Titanium Dioxide (TiO2) Nanomaterials. *Chem. Rev.* **2014**, *114* (19), 9281–9282. https://doi.org/10.1021/cr500422r.

(3) Binas, V.; Venieri, D.; Kotzias, D.; Kiriakidis, G. Modified TiO2 Based Photocatalysts for Improved Air and Health Quality. *Journal of Materiomics*. Chinese Ceramic Society March 1, 2017, pp 3–16. https://doi.org/10.1016/j.jmat.2016.11.002.

(4) Fujishima, A.; Rao, T. N.; Tryk, D. A. Titanium Dioxide Photocatalysis. *J. Photochem. Photobiol. C Photochem. Rev.* **2000**, *1* (1), 1–21. https://doi.org/10.1016/S1389-5567(00)00002-2.

(5) Qian, R.; Zong, H.; Schneider, J.; Zhou, G.; Zhao, T.; Li, Y.; Yang, J.; Bahnemann, D. W.; Pan, J. H. Charge Carrier Trapping, Recombination and Transfer during TiO2 Photocatalysis: An Overview. *Catal. Today* **2019**, *335*, 78–90. https://doi.org/10.1016/j.cattod.2018.10.053.

(6) Sun, J.; Guo, L. H.; Zhang, H.; Zhao, L. UV Irradiation Induced Transformation of TiO2 Nanoparticles in Water: Aggregation and Photoreactivity. *Environ. Sci. Technol.* **2014**, *48* (20), 11962–11968. https://doi.org/10.1021/es502360c.

(7) Wang, P.; Qi, N.; Ao, Y.; Hou, J.; Wang, C.; Qian, J. Effect of UV Irradiation on the

Aggregation of TiO2 in an Aquatic Environment: Influence of Humic Acid and PH. *Environ. Pollut.* **2016**, *212*, 178–187. https://doi.org/10.1016/j.envpol.2016.01.030.

(8) Zhang, H.; Sun, J.; Guo, L. H. UV Irradiation Mediated Aggregation of TiO2 Nanoparticles in Simulated Aquatic System. *NanoImpact* **2016**, *3–4*, 75–80. https://doi.org/10.1016/j.impact.2016.08.004.

(9) Gurr, J.-R.; Wang, A. S. S.; Chen, C.-H.; Jan, K.-Y. Ultrafine Titanium Dioxide Particles in the Absence of Photoactivation Can Induce Oxidative Damage to Human Bronchial Epithelial Cells. *Toxicology* **2005**, *213* (1–2), 66–73. https://doi.org/10.1016/j.tox.2005.05.007.

(10) Jugan, M. L.; Barillet, S.; Simon-Deckers, A.; Sauvaigo, S.; Douki, T.; Herlin, N.; Carrière, M. Cytotoxic and Genotoxic Impact of TiO2 Nanoparticles on A549 Cells. *J. Biomed. Nanotechnol.* **2011**, *7* (1), 22–23.

(11) Jayaram, D. T.; Kumar, A.; Kippner, L. E.; Ho, P. Y.; Kemp, M. L.; Fan, Y.; Payne, C. K. TiO2 Nanoparticles Generate Superoxide and Alter Gene Expression in Human Lung Cells. *RSC Adv.* **2019**, *9* (43), 25039–25047. https://doi.org/10.1039/c9ra04037d.

(12) Uchino, T.; Tokunaga, H.; Ando, M.; Utsumi, H. Quantitative Determination of OH Radical Generation and Its Cytotoxicity Induced by TiO(2)-UVA Treatment. *Toxicol. In Vitro* **2002**, *16* (5), 629–635. https://doi.org/10.1016/s0887-2333(02)00041-3.

(13) Wang, C.; Cao, S.; Tie, X.; Qiu, B.; Wu, A.; Zheng, Z. Induction of Cytotoxicity by Photoexcitation of TiO2 Can Prolong Survival in Glioma-Bearing Mice. *Mol. Biol. Rep.* **2011**, *38* (1), 523–530. https://doi.org/10.1007/s11033-010-0136-9.

(14) Gopalan, R. C.; Osman, I. F.; Amani, A.; De Matas, M.; Anderson, D. The Effect of Zinc Oxide and Titanium Dioxide Nanoparticles in the Comet Assay with UVA Photoactivation of Human Sperm and Lymphocytes. *Nanotoxicology* **2009**, *3* (1), 33–39. https://doi.org/10.1080/17435390802596456.

(15) Warheit, D. B.; Webb, T. R.; Sayes, C. M.; Colvin, V. L.; Reed, K. L. Pulmonary Instillation Studies with Nanoscale TiO2 Rods and Dots in Rats: Toxicity Is Not Dependent upon Particle Size and Surface Area. *Toxicol. Sci.* **2006**, *91* (1), 227–236. https://doi.org/10.1093/toxsci/kfj140.

(16) Nemmar, A.; Melghit, K.; Ali, B. H. The Acute Proinflammatory and Prothrombotic Effects of Pulmonary Exposure to Rutile TiO_2 Nanorods in Rats. *Exp. Biol. Med.* **2008**, *233* (5), 610–619. https://doi.org/10.3181/0706-RM-165.

(17) Li, Y. S.; Ootsuyama, Y.; Kawasaki, Y.; Morimoto, Y.; Higashi, T.; Kawai, K. Oxidative DNA Damage in the Rat Lung Induced by Intratracheal Instillation and Inhalation of Nanoparticles. *J. Clin. Biochem. Nutr.* **2018**, *62* (3), 238–241. https://doi.org/10.3164/jcbn.17-70.

(18) Introduction to Solar Radiation https://www.newport.com/t/introduction-to-solar-radiation (accessed Jul 20, 2020).

(19) Petković, J.; Küzma, T.; Rade, K.; Novak, S.; Filipič, M. Pre-Irradiation of Anatase TiO 2 Particles with UV Enhances Their Cytotoxic and Genotoxic Potential in Human Hepatoma HepG2 Cells. *J. Hazard. Mater.* **2011**, *196*, 145–152. https://doi.org/10.1016/j.jhazmat.2011.09.004.

(20) Hurum, D. C.; Agrios, A. G.; Gray, K. A.; Rajh, T.; Thurnauer, M. C. Explaining the Enhanced Photocatalytic Activity of Degussa P25 Mixed-Phase TiO2 Using EPR. *J. Phys. Chem. B* **2003**, *107* (19), 4545–4549. https://doi.org/10.1021/jp0273934.

(21) Janus, M.; Morawski, A. W. New Method of Improving Photocatalytic Activity of Commercial Degussa P25 for Azo Dyes Decomposition. *Applied Catalysis B: Environmental*. Elsevier August 29, 2007, pp 118–123. https://doi.org/10.1016/j.apcatb.2007.04.003.

(22) Du, P.; Bueno-López, A.; Verbaas, M.; Almeida, A. R.; Makkee, M.; Moulijn, J. A.;

Mul, G. The Effect of Surface OH-Population on the Photocatalytic Activity of Rare Earth-Doped P25-TiO2 in Methylene Blue Degradation. *J. Catal.* **2008**, *260* (1), 75–80. https://doi.org/10.1016/j.jcat.2008.09.005.

(23) Chen, D. W.; Shi, J. E.; Yan, J. C.; Wang, Y. H.; Yan, F. C.; Shang, S. X.; Xue, J. Controllable Synthesis of Titania Nanocrystals with Different Morphologies and Application to the Degradation of Phenol. *Chem. Res. Chinese Univ.* **2008**, *24* (3), 362–366. https://doi.org/10.1016/S1005-9040(08)60076-8.

(24) Zhao, J.; Milanova, M.; Warmoeskerken, M. M. C. G.; Dutschk, V. Surface Modification of TiO2 Nanoparticles with Silane Coupling Agents. *Colloids Surfaces A Physicochem. Eng. Asp.* **2012**, *413*, 273–279. https://doi.org/10.1016/j.colsurfa.2011.11.033.

(25) Fujishima, A.; Zhang, X. Titanium Dioxide Photocatalysis: Present Situation and Future Approaches. *Comptes Rendus Chimie*. **2006**, *9*(5-6), 750–760. https://doi.org/10.1016/j.crci.2005.02.055.

(26) Hashimoto, K.; Irie, H.; Fujishima, A. TiO 2 Photocatalysis: A Historical Overview and Future Prospects. *Jpn. J. Appl. Phys.* **2005**, *44* (12), 8269–8285.

(27) Sendra, M.; Moreno-Garrido, I.; Yeste, M. P.; Gatica, J. M.; Blasco, J. Toxicity of TiO2, in Nanoparticle or Bulk Form to Freshwater and Marine Microalgae under Visible Light and UV-A Radiation. *Environ. Pollut.* **2017**, *227*, 39–48. https://doi.org/10.1016/j.envpol.2017.04.053.

(28) Guidelines on Limits of Exposure to Ultraviolet Radiation of Wavelengths between 180 Nm and 400 Nm (Incoherent Optical Radiation). The International Non-Ionizing Radiation Committee of the International Radiation Protection Association. *Health Phys.* **1985**, *49* (2), 331–340.

(29) Kose, O.; Tomatis, M.; Leclerc, L.; Belblidia, N. B.; Hochepied, J. F.; Turci, F.; Pourchez, J.; Forest, V. Impact of the Physicochemical Features of TiO2Nanoparticles

on Their in Vitro Toxicity. *Chem. Res. Toxicol.* **2020**, *33* (9), 2324–2337. https://doi.org/10.1021/acs.chemrestox.0c00106.

(30) Wang, S.; Yu, H.; Wickliffe, J. K. Limitation of the MTT and XTT Assays for Measuring Cell Viability Due to Superoxide Formation Induced by Nano-Scale TiO 2. *Toxicol. Vitr.* **2011**, *25* (8), 2147–2151. https://doi.org/10.1016/j.tiv.2011.07.007.

(31) Marucco, A.; Fenoglio, I.; Turci, F.; Bice, F. Interaction of Fibrinogen and Albumin with Titanium Dioxide Nanoparticles of Different Crystalline Phases. *J. Phys. Conf. Ser. Nanosafe 2012 Int. Conf. Safe Prod. Use Nanomater. 13–15 Novemb. 2012, Grenoble, Fr.* **2013**, *429*, 012014. https://doi.org/10.1088/1742-6596/429/1/012014.

(32) Kwon, O. J.; Au, B. T.; Collins, P. D.; Adcock, I. M.; Mak, J. C.; Robbins, R. R.; Chung, K. F.; Barnes, P. J. Tumor Necrosis Factor-Induced Interleukin-8 Expression in Cultured Human Airway Epithelial Cells. *Am. J. Physiol.* **1994**, *267* (4 Pt 1), L398-405. https://doi.org/10.1152/ajplung.1994.267.4.L398.

(33) Mittelman, A. M.; Fortner, J. D.; Pennell, K. D. Effects of Ultraviolet Light on Silver Nanoparticle Mobility and Dissolution. *Environ. Sci. Nano* **2015**, *2* (6), 683–691. https://doi.org/10.1039/c5en00145e.

(34) Cho, M.; Chung, H.; Choi, W.; Yoon, J. Linear Correlation between Inactivation of E. Coli and OH Radical Concentration in TiO2 Photocatalytic Disinfection. *Water Res.* **2004**, *38* (4), 1069–1077. https://doi.org/10.1016/j.watres.2003.10.029.

(35) Xiong, S.; George, S.; Ji, Z.; Lin, S.; Yu, H.; Damoiseaux, R.; France, B.; Ng, K. W.; Loo, S. C. J. Size of TiO2 Nanoparticles Influences Their Phototoxicity: An in Vitro Investigation. *Arch. Toxicol.* **2013**, *87* (1), 99–109. https://doi.org/10.1007/s00204-012-0912-5.

(36) George, S.; Pokhrel, S.; Ji, Z.; Henderson, B. L.; Xia, T.; Li, L.; Zink, J. I.; Nel, A. E.; Mädler, L. Role of Fe Doping in Tuning the Band Gap of TiO2 for the Photo-Oxidation-

Induced Cytotoxicity Paradigm. *J. Am. Chem. Soc.* **2011**, *133* (29), 11270–11278. https://doi.org/10.1021/ja202836s.

(37) Dekali, S.; Divetain, A.; Kortulewski, T.; Vanbaelinghem, J.; Gamez, C.; Rogerieux, F.; Lacroix, G.; Rat, P. Cell Cooperation and Role of the P2X7 Receptor in Pulmonary Inflammation Induced by Nanoparticles. *Nanotoxicology* **2013**, *7* (8), 1302–1314. https://doi.org/10.3109/17435390.2012.735269.

(38) Mittal, M.; Siddiqui, M. R.; Tran, K.; Reddy, S. P.; Malik, A. B. Reactive Oxygen Species in Inflammation and Tissue Injury. *Antioxidants and Redox Signaling*. Mary Ann Liebert, Inc. March 1, 2014, pp 1126–1167. https://doi.org/10.1089/ars.2012.5149.

(39) Vaziri, N. D.; Rodríguez-Iturbe, B. Mechanisms of Disease: Oxidative Stress and Inflammation in the Pathogenesis of Hypertension. *Nature Clinical Practice Nephrology*. Nature Publishing Group October 14, 2006, pp 582–593. https://doi.org/10.1038/ncpneph0283.

(40) Jugan, M. L.; Barillet, S.; Simon-Deckers, A.; Sauvaigo, S.; Douki, T.; Herlin, N.; Carrière, M. Cytotoxic and Genotoxic Impact of TiO_2 Nanoparticles on A549 Cells. *J. Biomed. Nanotechnol.* **2011**, *7* (1), 22–23. https://doi.org/10.1166/jbn.2011.1181.

(41) Simon-Deckers, A.; Gouget, B.; Mayne-L'Hermite, M.; Herlin-Boime, N.; Reynaud, C.; Carrière, M. In Vitro Investigation of Oxide Nanoparticle and Carbon Nanotube Toxicity and Intracellular Accumulation in A549 Human Pneumocytes. *Toxicology* **2008**, *253* (1–3), 137–146. https://doi.org/10.1016/J.TOX.2008.09.007.

(42) Heffner, J. E.; Repine, J. E. Pulmonary Strategies of Antioxidant Defense. *Am. Rev. Respir. Dis.* **1989**, *140* (2), 531–554. https://doi.org/10.1164/ajrccm/140.2.531.

(43) Kim, J. K.; Lee, W. K.; Lee, E. J.; Cho, Y. J.; Lee, K. H.; Kim, H. S.; Chung, Y.; Kim, K. A.; Lim, Y. Mechanism of Silica- and Titanium Dioxide-Induced Cytotoxicity in Alveolar Macrophages. *J. Toxicol. Environ. Heal. - Part A* **1999**, *58* (7), 437–450.

https://doi.org/10.1080/009841099157160.

(44) Reeves, J. F.; Davies, S. J.; Dodd, N. J. F.; Jha, A. N. Hydroxyl Radicals ({radical Dot}OH) Are Associated with Titanium Dioxide (TiO2) Nanoparticle-Induced Cytotoxicity and Oxidative DNA Damage in Fish Cells. *Mutat. Res. - Fundam. Mol. Mech. Mutagen.* **2008**, *640* (1–2), 113–122. https://doi.org/10.1016/j.mrfmmm.2007.12.010.

(45) Cai, R.; Kubota, Y.; Shuin, T.; Sakai, H.; Hashimoto, K.; Fujishima2, A. *Induction of Cytotoxicity by Photoexcited TiO2 Particles'*; 1992.

(46) Nam, Y.; Lim, J. H.; Ko, K. C.; Lee, J. Y. Photocatalytic Activity of TiO2 Nanoparticles: A Theoretical Aspect. *Journal of Materials Chemistry A*. Royal Society of Chemistry 2019, pp 13833–13859. https://doi.org/10.1039/c9ta03385h.

(47) Jeon, S.; Clavadetscher, J.; Lee, D.-K.; Chankeshwara, S. V; Bradley, M.; Cho, W.-S. Surface Charge-Dependent Cellular Uptake of Polystyrene Nanoparticles. *Nanomater. (Basel, Switzerland)* **2018**, *8* (12). https://doi.org/10.3390/nano8121028.

(48) Beck, M.; Mandal, T.; Buske, C.; Lindén, M. Serum Protein Adsorption Enhances Active Leukemia Stem Cell Targeting of Mesoporous Silica Nanoparticles. *ACS Appl. Mater. Interfaces* **2017**, *9* (22), 18566–18574. https://doi.org/10.1021/acsami.7b04742.

(49) Chen, D.; Ganesh, S.; Wang, W.; Amiji, M. Plasma Protein Adsorption and Biological Identity of Systemically Administered Nanoparticles. *Nanomedicine*. Future Medicine Ltd. September 1, 2017, pp 2113–2135. https://doi.org/10.2217/nnm-2017-0178.

(50) Forest, V.; Pourchez, J. Preferential Binding of Positive Nanoparticles on Cell Membranes Is Due to Electrostatic Interactions: A Too Simplistic Explanation That Does Not Take into Account the Nanoparticle Protein Corona. *Materials Science and Engineering C*. Elsevier Ltd January 1, 2017, pp 889–896. https://doi.org/10.1016/j.msec.2016.09.016.

(51) Lesniak, A.; Salvati, A.; Santos-Martinez, M. J.; Radomski, M. W.; Dawson, K. A.; Åberg, C. Nanoparticle Adhesion to the Cell Membrane and Its Effect on Nanoparticle Uptake Efficiency. *J. Am. Chem. Soc.* **2013**, *135* (4), 1438–1444. https://doi.org/10.1021/ja309812z.

(52) Forest, V. CHAPTER 2: Biological Significance of the Nanoparticles Protein Corona. In *Issues in Toxicology*; Royal Society of Chemistry, 2019; Vol. 2019-January, pp 31–60. https://doi.org/10.1039/9781788016308-00031.